

American University in Cairo

AUC Knowledge Fountain

Faculty Journal Articles

7-6-2023

Lutein and β -Carotene Characterization in Free and Nanodispersion Forms in Terms of Antioxidant Activity and Cytotoxicity

Nourhan S. Elkholy

Mohamad Louai M. Hariri

Haitham S. Mohammed

Medhat W. Shafaa

Follow this and additional works at: https://fount.aucegypt.edu/faculty_journal_articles

Recommended Citation

APA Citation

Elkholy, N. Hariri, M. Mohammed, H. & Shafaa, M. (2023). Lutein and β -Carotene Characterization in Free and Nanodispersion Forms in Terms of Antioxidant Activity and Cytotoxicity. *Journal of Pharmaceutical Innovation*, 18, 1727–1744. [10.1007/s12247-023-09745-2](https://doi.org/10.1007/s12247-023-09745-2)
https://fount.aucegypt.edu/faculty_journal_articles/5237

MLA Citation

Elkholy, Nourhan S., et al. "Lutein and β -Carotene Characterization in Free and Nanodispersion Forms in Terms of Antioxidant Activity and Cytotoxicity." *Journal of Pharmaceutical Innovation*, vol. 18, 2023, pp. 1727–1744.
https://fount.aucegypt.edu/faculty_journal_articles/5237

This Research Article is brought to you for free and open access by AUC Knowledge Fountain. It has been accepted for inclusion in Faculty Journal Articles by an authorized administrator of AUC Knowledge Fountain. For more information, please contact fountadmin@aucegypt.edu.

Lutein and β -carotene characterization in free and nanodispersion forms in terms of antioxidant activity and cytotoxicity

Nourhan Elkholy (✉ phy.nsayed@gmail.com)

Helwan University Faculty of Science <https://orcid.org/0000-0001-7344-5922>

Mohamad Louai M. Hariri

Haitham S. Mohammed

Medhat W. Shafaa

Research Article

Keywords: Lutein, β -carotene, Nanodispersion, Tween 80, Antioxidant assay, Cytotoxicity

Posted Date: January 20th, 2023

DOI: <https://doi.org/10.21203/rs.3.rs-2485101/v1>

License: © ⓘ This work is licensed under a Creative Commons Attribution 4.0 International License. [Read Full License](#)

Version of Record: A version of this preprint was published at Journal of Pharmaceutical Innovation on July 6th, 2023. See the published version at <https://doi.org/10.1007/s12247-023-09745-2>.

Abstract

Purpose: Carotenoids are potent natural antioxidants with many important applications. Their nanodispersion formulations can solve problems that may limit their usage. In this study, we produced carotenoid nanodispersions from extracted lutein (Nano-Lut), extracted β -carotene (Nano-EBc), and synthetic β -carotene (Nano-SBC).

Methods: The present study has quantitatively emphasized the physicochemical, antioxidant, and cytotoxic properties of free and nanodispersed formulations of lutein and β -carotene. The nanodispersions were characterized by spectral absorption, dynamic light scattering, and zeta potential. Antioxidant and cytotoxicity assays were conducted for free and their nanodispersed forms. The cytotoxicity of free carotenoids and their nanodispersions was conducted on HSF, VERO, and BNL cell lines.

Results: Nano-Lut has the smallest mean particle size (185.2 ± 40.5 nm, PDI of 0.183 ± 0.01 , and zeta potential of -28.6 ± 6.4 mV). Nano-SBc showed monomodal size distribution (220.5 ± 30.09 nm, PDI of 0.318 ± 0.03 , and zeta potential of -12.1 ± 5.9 mV), while Nano-EBc showed a bimodal size distribution (with a mean particle size of 498.3 ± 88.9 nm, PDI of 0.65 ± 0.08 , and zeta potential of -39.7 ± 1.3 mV). All prepared nanodispersions showed less than 20% loss during the formulation process. Antioxidant assays showed that extracted lutein was the most active and synthetic β -carotene was the least. Cells showed higher tolerance for lutein and its nanodispersion than extracted or synthetic β -carotene either in free or nanodispersion forms.

Conclusions: The study proved that lutein in nanodispersed form possesses the smallest size, the highest antioxidant activity, and the lowest cytotoxicity among the tested formulations.

Introduction

Carotenoids are lipophilic substances found in bacteria, fungi, algae, and plant biomass [1-3]. They are synthesized and sequestered in plastids, where they are stored in a lipophilic environment [4]. Nevertheless, carotenoids are essential for several biological processes and protection from serious illnesses like cancer [1-3,5,6], age-related macular degeneration [1-3,6], and cardiovascular disorders [2,3,6], the human body cannot produce them on its own [2,3]. Since many fruits and vegetables high in carotenoids are not consumed in amounts that allow their carotenoid content to execute their functions effectively, some dietary carotenoids are insufficient in our food intake and should be supplemented [1-3, 6]. Carotenoids are added to animal food [4-6], pharmaceuticals [2-6], food coloring [1], and vitamin supplements [1-6].

Due to their capacity to scavenge many forms of free radicals, carotenoids are well-known to be effective antioxidant reagents [1-3,5,6]. They can also regulate gap junction communications between cells [2,4-8]. They have a wide range of impacts on cell proliferation [2,4,6], modulate transcriptional activity [5,6,8], and control the cell cycle [4,6,7]. Furthermore, carotenoids improve overall health and lower the risk of diseases [1-6] such as prostate [1,4,6-8], breast [1,6], cervical, ovarian [7], and colorectal cancer [4-8], metabolic disorders like diabetes mellitus and obesity [2,6,7], as well as diseases related to the bone [6,7], skin [6-8], and eyes [2,3,6-8], and as mental decline [6]. However, this healing power depends on many variables,

including their concentration and availability in the target cells, tissues, or cellular compartments and the free radicals' type [1, 4-8].

There are few reported exceptions to the notion that carotenoids often are harmless, even when used at elevated levels as pure supplements [1,2]. Canthaxanthin at high concentrations can cause reversible retinopathy [1]. Additionally, smokers should avoid consuming enormous amounts of Bc (20–30 mg/d in supplement form) due to the increased risk of stomach and lung cancers [1]. Furthermore, consuming too high quantities of carotenoids can cause carotenemia, which causes reversible skin yellowing [1].

Human fluids (plasma, milk, and semen) and tissues contain carotenoids as geometrical cis/trans isomers in their free forms rather than ester forms. The liver, adrenals, adipose tissue, scalp, breast tissue, cervix, colon, eye, and brain were among the sites where carotenoids were found. That wide distribution emphasizes the bioavailability of carotenoids [6,7].

When getting carotenoids as a nutritional supplement, each stage of carotenoid intake influences absorption, causing a significant shift in the concentration of carotenoids in plasma and lymph, which impacts tissue and organ accumulation. Release from the dietary matrix, transformation to lipid droplets, integration into mixed bile salt micelles during ingestion, uptake and metabolism by enterocytes, and incorporation into chylomicrons for secretion into the lymph are the steps taking place in the absorption of carotenoids. As a result, the bioavailability and effectiveness of carotenoids in the food matrix may be disrupted. The kind of food matrix, sources, particle size, the way that food is processed, the quantity of accompanying dietary lipids, fiber, phytosterols, carotenoids type, the nutritional status, the physiological status as gut health, and the genotype of the consumer are just a few of the variables that affect how well carotenoids are absorbed from the food [1,4].

The double-bond conjugated system is the essential component of the molecule and is mostly accountable for its biological activity [1,3,6]. Hydrocarbon carotenoids, also known as carotenes, include β -carotene (Bc), lycopene, and α -carotene, whereas oxy-carotenoids, also known as xanthophylls, including lutein, zeaxanthin, and β -cryptoxanthin. [3,4,6]. Bc [Figure 1] with a molecular formula ($C_{40}H_{56}$), is one of the most efficient compounds known to quench singlet oxygen, raising the possibility that Bc may prevent cancer through an antioxidant mechanism [9]. It represents the major carotenoid of many foods (e.g., apricot, carrot, mango, loquat, West Indian Cherry, and palm fruits) [10]. One of the three provitamin A (retinol) forms is Bc. β -cryptoxanthin and α -carotene are the other two. Human carotenoid cleavage enzymes split Bc into two retinol molecules (vitamin A aldehydes) [11].

Lutein (Lut) got its name from the Latin luteus, which means yellow, and it means the yellow color of the leaves in Chinese. Lut is found with higher concentrations than zeaxanthin in leaves, green vegetables such as spinach and kale, and yellow flowers. The long linear aliphatic carbon chain provides Lut (β , ϵ -carotene-3,3'-diol) [Figure 1] the properties of an antioxidant, and as a blue light absorber, it appears as a yellow compound. Lut has a molecular formula, $C_{40}H_{56}O_2$. It is formed from eight isoprene units (tetraterpenoid) and two hydroxyl functional groups at the two ends [10,12].

Since carotenoids are lipophilic substances, they must be delivered to tissues through blood or plasma by carriers like lipoproteins [2,4,6]. They are eliminated very slowly; after 1-week supplementation with either Bc or Lut, plasma concentrations return to baseline after three weeks [2,4]. When two immiscible liquids, such as oil and water, are combined, the resulting solution is known as dispersion, in which the disperse phase is the phase that spreads as minute droplets into the other phase, which is known as the continuous phase [13]. Carotenoid nanodispersion enhances carotenoids' bioavailability and solubility in water and lipids (or oils). Nanodispersion often increases the surface-to-volume ratio by reducing particle size to the nanoscale range and alters its reactivity by several folds with changes in mechanical, electrical, and optical characteristics [14, 15].

Therefore, the objective of this study was to prepare nanodispersion of extracted lutein from marigold flowers (Nano-Lut), nanodispersion of extracted β -carotene from carrots (Nano-EBc), and nanodispersion of synthetic β -carotene (Nano-SBc) via the solvent displacement method using Tween 80 as a surfactant. The resulting nanodispersions were then characterized in terms of drug content percentage, absorption spectra, zeta potential value, particle size, and polydispersity index. The work extended to investigate the antioxidant activities of these prepared nanodispersions in comparison to their free forms as well as to evaluate the cytotoxic properties of these nanodispersions on selected normal cell lines.

Materials And Methods

Chemicals

Carotenoids reference standards and synthetic β -carotene ($\geq 97\%$) were purchased from Sigma (St. Louis, Mo, USA). Solutions were prepared in ultra-pure deionized water. Marigold flowers and carrots were purchased from local markets in Egypt. All other used reagents were of high purity and solvents were of HPLC grade.

Carotenoids Extraction, Purification, Identification

Extraction of Lutein from

Marigold flower (*Tagetes erecta* L.)

A summary of lutein extraction from marigold petals is shown in **Figure 2**. The Orange Marigold flower (*Tagetes erecta* L.) was selected after evaluating some available yellow and orange *Tagetes* types. It was found that the orange Marigold flower contains the highest amount of trans-lutein and lutein esters [16]. The darker the color of the flowers, the more lutein and lutein esters they contain. Flowers were picked, and then only petals were used [17].

Petals were dried in the shade to remove the water content for 2-3 days (dehydration) because water decreases extraction efficiency. Then they were crushed using a pestle and mortar. In a separate flask, a 300 ml mixture of methanol, hexane, and ethyl acetate (1:1:1) was prepared and mixed with a magnetic stirrer with 50 ml of 15% methanolic potassium hydroxide. 10 g Petals were added to the organic mixture

and stirred for 30 min at room temperature. After that, the mixture was filtered, and the petals were soaked again with a new solvent solution to extract all the pigments from the flowers. This step was repeated until the petals changed to deep brown color [18-21].

The red-orange extract solution was collected and evaporated using a rotary evaporator at 40 °C to evaporate the organic solvents without degrading the carotenoids. The extract was collected by dissolving it in diethyl ether, transferred into a separating funnel, and washed with NaCl-saturated water (1:1) until obtaining unturbid layers. The Diethyl ether layer was filtered on anhydrous sodium sulfate to remove the moisture, to obtain marigold oleoresin [18-20].

The oleoresin was dried using a rotary evaporator and collected with 50 ml diethyl ether. Then 50 ml of 20% methanolic potassium hydroxide was added to liberate the carotenoids from their ester linkage with fatty acids. This flask was left stirring at room temperature and monitored by thin layer chromatography (TLC) every 20 min to check the reaction. The reaction was stopped when the esters bands disappeared. After completing the saponification process, the mixture evaporated, and the residue was collected with diethyl ether. The extract was washed with saturated NaCl water again (1:1) to separate the pearl-white precipitate [18-21]. After dehydration with anhydrous sodium sulfate, the sample was concentrated by a rotary evaporator attached to a vacuum pump with water bathing at a temperature not exceeding 40 °C.

Purification of extracted lutein

A glass open gravity column (15×250 mm) was used for a preliminary study of lutein purification solvents and ratios. Finally, it was packed with silica gel slurry, and 0.5 ml of extract stock solution in hexane was loaded into the column. A gradient ratio of hexane and acetone was used to allow the fractions to flow [22].

Puriflash helps sample separation on a large scale and increases the purity in the final separation step. Marigold extract was dissolved in ethyl acetate and mixed with silica to the ratio of 1:3 (w/w). The suspension was evaporated using a rotatory evaporator adjusted at 40 °C to evaporate the solvent and load the extract. The dry-loaded extract was chromatographed using the same gradient solvent system used in the preliminary open column by Puriflash (4100, INTERCHIM Co., France) with a PDA-UV-Vis 190 – 840 nm detector with 22 bars pump and flow rate 10 ml/min on Silica HP 30 µm–25 g. The gradient elution is summarized in **Table 1**.

The peaks were separately collected and evaluated on TLC against standard lutein using the 80:20 ratio (hexane to acetone) mobile phase and, accordingly, the band, which was found to have the same retention factor (RF) value as the standard and the characteristic UV-Vis spectrum, was collected. Then the band evaporated and stored at -20 in an amber-colored vial. Lutein started to elute at the hexane-to-acetone ratio of 80:20.

Table 1: The gradient elution for lutein purification using Puriflash in terms of column Volume (CV) and the hexane/acetone ratio.

Column Volume (CV)	Hexane %	Acetone%
0	100	0
5	100	0
15	90	10
25	85	15
35	80	20
55	80	20
55.1	0	100
60	0	100

Extraction of β -carotene from carrots (*Daucus carota* L.)

β -carotene is readily soluble in dichloromethane [23]. Therefore, the following extraction technique was applied according to Rifqi et al. [24] with modifications. 100 g of carrots were washed with distilled water and cut into small pieces. Carrot pieces were dried in the shade to remove the water content for 2-3 days (dehydration). After drying, the carrot pieces were mashed using a blender, and the carrot mass was mixed with dichloromethane to a ratio of 1:10 (w/v). The mixture was homogenized using Ultraturrax T50 IKA Labortechnik and shaft number G45ME for 15 minutes with a pause of 5 minutes at each interval at 4000 rpm. After collecting the filtrate, the homogenization step was repeated 4 times.

The extract filtrates were collected and concentrated using a rotatory evaporator at 40 °C under a vacuum. Then the concentrated extract was dissolved in dichloromethane and washed with saturated NaCl in distilled water (1:1) several times until obtaining unturbid layers. The organic layer was filtered on anhydrous sodium sulfate. Then the solvent was evaporated under a vacuum using a rotatory evaporator at 40 °C to obtain carrot oleoresin.

Purification of extracted of β carotene

β -carotene purification was conducted with similar steps to lutein purification, considering the difference in the component nature and polarity. The carrot extract was dissolved in dichloromethane and mixed with silica to the ratio of 1:3 (w/w). The suspension was evaporated using a rotatory evaporator adjusted at 40 °C to evaporate the solvent and load the extract for flash chromatography purification on Puriflash. The same conditions were applied except for the mobile phase composition, which involved 100% hexane, and the flow rate was set at 5 ml/min. The column-washing step was conducted using 100% acetone. The peaks were separately collected and assessed on TLC against standard Bc using the same mobile phase. Accordingly, the band was found to have the same RF value as the standard, and the characteristic UV-Vis spectrum was determined. Then the band evaporated and stored at -20 in an amber-colored vial.

Carotenoids Identification

A compact Mass Spectrometer APCI (TLC-MS, Advion, USA), high-performance liquid chromatography (HPLC) [Waters 2695 LC, 996 PDA detector, pump with a low-pressure mixing system, auto-sampler with a

sample loop of 100 µl, and a reversed-phase C18 column Scharlau (250 x 4,6mm), 5 µm.], and nuclear magnetic resonance (NMR) [Bruker Avance HDIII 400 MHz, Czechia] were used to identify Lut, EBc, and SBc. The methods used and results were provided in detail in the supplementary information section.

Nanodispersions

Preparation

Extracted lutein nanodispersions (Nano-Lut), extracted β-carotene nanodispersions (Nano-EBc), and synthetic β-carotene nanodispersions (Nano-SBc) were prepared using the solvent displacement method. Samples of Lut, SBc, and EBc were scanned using the spectrophotometer (v-630, JASCO, Spain) to take the needed amount according to the following effective weight equation:

$$W(\text{mg}) = \frac{A \times V \times 10^3}{A_{1\text{cm}}^{1\%} \times 100} \times \text{DF}$$

where, A: Absorbance, V: Stock volume, $A_{1\text{cm}}^{1\%}$: Specific Extinction Coefficient (Depending on the solvent and the kind of carotenoids), and DF: Dilution Factor.

For Nano-Lut, two stocks were made: one containing 0.1% (w/w%) Tween 80 (T80) in deionized water, which served as the aqueous phase, and the other containing 0.1% (w/w%) Lut in acetone, which served as the organic phase (acetone's density is 0.791 g/ml). A one-shot addition of the organic phase at a volume ratio of 1:9 to the aqueous phases was made. A magnetic stirrer was used to mix them for 30 minutes at 750 rpm. A rotary evaporator (Re-2010, Lanphan Zhengzhou, Henan, China) was then used to remove the acetone for 30 minutes at 40 °C and 60 rpm [25-28].

To create Nano-SBc or Nano-EBc, two stocks were made: one containing 1% (w/w%) T80 in deionized water and the other 0.2% (w/w%) Bc in hexane (hexane's density is 0.655 g/ml). The same procedures were carried out as the previous procedure. However, the organic to the aqueous phase was dropwise added [15, 29-31]. Many trials were assessed, and the parameters that resulted in the smallest size and highest drug content were chosen (data not shown).

Drug Content Measurement

The determination of drug content was performed by extraction method according to Tan et al. [25] with some modifications. Aliquots of 1 ml carotenoid nanodispersion and 3 ml dichloromethane were vortexed vigorously for 3 min at room temperature to get the untrapped quantity of carotenoids in the dispersion. The mixture was centrifuged at 3000 g for 5 minutes to collect the supernatant. This action was conducted twice. The gathered supernatant was then diluted with dichloromethane in a tube. Using dichloromethane as the blank, the untrapped quantity of carotenoids was spectrophotometrically quantized at 460 and 452 nm for Bc and Lut, respectively. Each experiment was conducted in an independent triplet. Carotenoids'

drug content in nanodispersions was determined by dividing the concentration of carotenoids recovered by extraction by the total concentration required to prepare the nanodispersion [23, 25].

Dynamic Light Scattering Measurement

The mean particle size and size distribution of freshly prepared nanodispersions were determined by the dynamic light scattering using a particle sizing system (Zetasizer Nano ZS, Malvern, UK) at 25 °C. The results were expressed as the average of three independent measurements.

Zeta Potential Measurements

The zeta potential of freshly prepared samples was determined in ultra-pure deionized water at 25 °C using Zetasizer Nano ZS, Malvern, UK. The results were expressed as the average of three individual measurements.

UV-visible Absorption Spectrometry

Spectrophotometry is considered an identification step because carotenoids have a characteristic spectrum in the UV-visible range. Free carotenoids were dissolved in methanol with a methanol blank. The deionized water was used as a blank of freshly prepared nanodispersions to determine their spectra using a spectrophotometer (spectrophotometer v-630, JASCO, Spain).

Antioxidants activities

ABTS

The assay was performed according to the method of Arnao, et al. [32], with minor modifications to be done in microplates. Briefly, ABTS reagent was prepared at a concentration of 7mM in distilled water. Then, 1mL of the solution was added to 17 µL of 140 mM potassium persulphate, and the mixture was left in the dark for 24 hours. 1 mL of the reaction mixture was then completed to 50 mL with methanol to obtain the final ABTS dilution used in the assay. 190 µL of freshly prepared ABTS reagent was mixed with 10 µL of the sample in 96 wells plate (n=6), and the reaction was incubated at room temperature for 30 minutes in a dark chamber. At the end of incubation time, the decrease in ABTS color intensity was measured at 734 nm. Data were represented as means ± SD according to the following equation:

Percentage inhibition = ((Average absorbance of blank - Average absorbance of the sample) / (Average absorbance of blank)) *100.

Free carotenoids were dissolved and blanked with methanol whereas nanodispersions were dispersed in water and blanked with it according to their effective concentration. Different concentrations of standard Trolox in methanol and another in water were evaluated in the same way to establish a standard linear curve between Trolox concentration and % inhibition of ABTS radical achieved at each concentration to calculate Trolox equivalent antioxidant capacity (TEAC).

Ferric-reducing antioxidant power (FRAP)

The assay was conducted according to the method of Benzie, et al. [33], with minor modifications to be conducted in microplates. Briefly, 2,4,6-Tris(2-pyridyl)-s-triazine (TPTZ) reagent was dissolved in 40mM HCl to obtain a concentration of 10mM. FeCl₃ solution was prepared at a concentration of 20mM in distilled water. On the day of analysis, TPTZ, FeCl₃, and acetate buffer (300mM pH=3.6) were added in the ratio 1:1:10 v/v/v. From this freshly prepared solution, 190 µL was mixed with 10 µL of the sample in 96 wells plate (n=6), and the reaction was incubated at room temperature for 30 min in the dark. At the end of the incubation period, the resulting blue color was measured at 593nm. Data were represented as means ± SD according to the following equation:

$$\text{Percentage inhibition} = ((\text{Average absorbance of blank} - \text{average absorbance of the sample}) / (\text{Average absorbance of blank})) * 100$$

Free carotenoids were dissolved and blanked with methanol wherever nanodispersions were dispersed in water and blanked with it according to their effective concentration. Different concentrations of standard Trolox in methanol and another in water were evaluated in the same way to establish standard linear curves between Trolox concentration and the absorbances obtained at each concentration to calculate TEAC.

Ferrozine

The assay was performed according to the method of Santos, et al. [34] with minor modifications to be conducted in microplates, briefly; 20 µL of the freshly prepared ferrous sulfate (0.3 mM in acetate buffer pH=6) was mixed with 50 µL of the sample in 96 wells of a plate (n=6). 30 µL of ferrozine (0.8 mM in acetate buffer pH=6) was then added to each well. The reaction mixture was incubated at room temperature for 10 minutes in the dark. At the end of incubation time, the decrease in the produced color intensity was measured at 562 nm. Data were represented as means ± SD according to the following equation:

$$\text{Percentage decrease} = ((\text{Average absorbance of blank} - \text{average absorbance of the sample}) / (\text{Average absorbance of blank})) * 100.$$

Free carotenoids were dissolved and blanked with methanol whereas nanodispersions were dispersed in water and blanked with it according to their effective concentration. Different concentrations of EDTA were evaluated in the same way to establish a standard linear curve between EDTA concentration and % inhibition of ferrozine-iron complex color achieved at each concentration to calculate EDTA equivalent antioxidant capacity.

DPPH

DPPH (2,2-diphenyl-1-picryl-hydrazyl-hydrate) free radical assay was conducted according to Boly, et al. [35]. Briefly, 100µL of freshly prepared DPPH reagent (1 mg in 10 mL methanol) was added to 100 µL of the tested sample and standard in 96 wells plate (n=6). Each sample was prepared at effective concentrations of 10 and 100 µM to screen its activity. Then six suitable effective concentrations were prepared for each

one to calculate the value of the IC₅₀. Free carotenoids were dissolved and blanked with methanol whereas nanodispersions were dispersed in water and blanked with it.

The reaction was incubated at room temp for 30 min in the dark. At the end of incubation time, the resulting reduction in DPPH color intensity was measured at 540 nm. Data are represented as means ± SD according to the following equation:

Percentage inhibition= ((Average absorbance of blank-average absorbance of the sample)/ (Average absorbance of blank)) *100.

Data were normalized using Microsoft Excel and the IC₅₀ value was calculated using Graph pad Prism 9. According to Zheng, et al. [36], the concentrations were converted into logarithmic values and a non-linear inhibitor regression equation (**log (inhibitor) vs. normalized response – variable slope equation**) was selected.

Oxygen Radical Absorbance Capacity (ORAC)

The assay was performed according to the method of Liang, et al. [37], with modifications. Briefly, in black plates, 10 µL of the prepared samples (according to their effective concentrations) was incubated with 30 µL fluoresceine (100 nM) for 10 min at 37 °C. Fluorescence measurement (485 EX nm, 520 nm EM) was conducted for three cycles (cycle time, 90 sec.) for background measurement. 70 µL of freshly prepared 2,2′Azobis (2-amidinopropane) dihydrochloride (AAPH) (300 mM) was added immediately to each well. Fluorescence measurement (485 nm EX, 520 nm EM) was continued for 60 min (40 cycles, each 90 sec). Data were represented as means (n=3) ± SD, and the compound's antioxidant activity was calculated as µM Trolox equivalents by substitution in the linear regression equation.

Cell culture and cytotoxicity assay

The HSF (Human Skin Fibroblast), VERO (Green Monkey Kidney), and BNL (Normal Mouse Liver Cells) cell lines were purchased from Nawah Scientific Inc. (Mokatam, Cairo, Egypt). Cells were kept alive in Dulbecco's Modified Eagle Medium (DMEM) supplemented with 10% heat-inactivated fetal bovine serum in a humidified, 100 mg/mL streptomycin, and 100 units/mL penicillin 5% (v/v) CO₂ atmosphere at 37 °C. The Sulforhodamine B (SRB) assay was used to measure cell viability. In 96-well plates, aliquots of a 100 µl cell suspension (5x10³ cells) were cultured in the medium for 24 hours. Another aliquot of 100 µL of medium containing different drug concentrations (µg/ml) was used to treat the cells. Free forms of carotenoids were dissolved in DMSO with a concentration used in each well of 0.2% DMSO of the total volume to avoid its toxicity. To evaluate whether the toxicity originated from the carotenoid or the vehicle; since the water content and surfactant can disrupt the cell membrane, the same volumes/ concentrations of water and T80 that were used to disperse the carotenoid were evaluated alone without incorporating the active carotenoid [38, 39].

Cells were fixed by changing the medium with 150 µL of 10% Trichloroacetic acid (TCA) and incubating at 4 °C for 1 hour after 48 hours of drug exposure. After the TCA solution was withdrawn, distilled water was

used to wash the cells five times. Aliquots of a 70 mL SRB solution (0.4% w/v) were added and then incubated for 10 min in a dark environment at room temperature. Plates were washed with 1% acetic acid three times and then left to air dry overnight. The protein-bound SRB stain was then dissolved using 150 L of TRIS (10 mM), and the absorbance was determined at 540 nm using a BMG LABTECH®- FLUOstar Omega microplate reader (Ortenberg, Germany) [38, 39].

Statistics

Results were expressed as the mean ± standard deviation. The significant difference ($P < 0.05$) between groups was evaluated by one-way analysis of variance (ANOVA) followed by the post hoc Tukey test.

Results

Carotenoids extraction, purification, and identification:

Lutein was successfully extracted from the marigold flower. Starting with 10 g of dried petals. It resulted in 0.55 g of marigold oleoresin which yielded ~ 100 mg (actual weight) and ~40 mg (effective weight) of Lut of all trans-lutein with purity exceeding 90% (detected by HPLC at 450 nm). Bc was successfully extracted from carrots. Starting with 100 g of carrots, resulted in 0.6 g of carrots oleoresin which yielded ~ 50 mg (actual weight) and ~15 mg (effective weight) of EBc as a mixture composed from 13-Cis isomer (~45%), all trans β carotene (~40%), and 9-Cis isomer (~10%) (detected by HPLC at 450 nm). Lut, EBc, and SBc were identified by TLC-mass, HPLC, and NMR. The results in detail were reported in the supplementary data.

Drug Content Results

The drug content % of the prepared nanodispersions exceeded 98.12 ± 0.88 , 80.1 ± 1.76 , and $94.8 \pm 0.22\%$ of Lut, EBc, and SBc, respectively.

Size Distribution and Zeta potential of Nanodispersions

Size distribution graphs for Nano-Lut, Nano-SBc, and Nano-EBc were shown in **Figure 3 A-C**. The size distribution of the Nano-Lut sample, as shown in **Figure 3A**, was concentrated around a mean particle size diameter of 185.2 ± 40.54 nm with a polydispersity index (PDI) of 0.183. The mean particle size diameter of Nano-SBc was 220.5 ± 30.09 nm with 0.318 PDI, as shown in **Figure 3B**. **Figure 3C** showed that the Nano-EBc has a mean size diameter of 498.3 ± 88.9 nm with 0.65 ± 0.08 PDI. The figure shows two peak maxima, with the first occurring at 160.6 ± 39.29 nm and the second at 790.7 ± 215.1 nm in diameter. The results of measurements of various nanodispersion formulations are summarized in **Table 2**.

Table 2: DLS, PDI, Zeta potential, and Drug content of various nanodispersions.

Sample	Size by DLS (nm)	PDI	Zeta potential (mV)	Drug Content (%)
Nano-Lut	185.2±40.54	0.183±0.01	-28.6±6.4	98.12±0.88
Nano-SBc	220.5±30.09	0.318±0.03	-12.1±5.9	94.8±0.22
Nano-EBc	498.3±88.9	0.65±0.08	-39.7±1.3	80.1±1.76

UV-Visible Spectroscopy

Figure 4 represents the absorption spectra of Lut and Bc in different molecular organization forms. **Figure 4A** displays the absorption spectrum of monomeric Lut in methanol, containing the three characteristic peaks for the $S_0 \rightarrow S_2$ transition, corresponding to the 0-0, 0-1, and 0-2 vibronic sub-levels, respectively. These transitions are numbered I, II, and III from short to long wavelengths. It represents the typical shape of the spectrum of Lut in a monomeric form, while the spectrum recorded by Nano-Lut in hydrated solution, blue-shifted and devoid of the vibrational substructure, represents the pigment molecules that are organized into the aggregated structure.

It was observed that the strongly allowed $S_0 \rightarrow S_2$ electronic transition of SBc monomer with vibronic features corresponds to 0-2, 0-1 and 0-0 transitions occurred in the 400-500 nm region, **Figure 4B**. The spectrum for Nano-SBc in aggregated form can be indicated in **Figure 4B**. The absorption spectrum of water nanodispersion of SBc was weakened in the 350–500 nm range. Spectroscopic variations of Nano-SBc (**Figure 4B**) could be good evidence for Nano-SBc synthesis. **Figure 4C** presents the absorption spectra of EBc in the same systems of methanol. It was also indicated from **Figure 4C** that Nano-EBc resulted in the formation of aggregated structures and was characterized by small spectral shifts. The absorption spectra of EBc and Nano-EBc were almost similar.

Antioxidant activity

Table 3 illustrates the antioxidant capacity results. In ORAC and ABTS, Lut has the best antioxidant capacity, where 1 μM of Lut (effective concentration) is equivalent to $26.507 \pm 2.112 \mu\text{M}$ and $4.546 \pm 0.320 \mu\text{M}$ of Trolox, respectively. When compared to EBc and SBc, whose 1 μM effective concentration was equal to 1.020 ± 0.078 and 0.662 ± 0.056 in ORAC and 4.066 ± 0.280 and $1.860 \mu\text{M}$ Trolox in ABTS, respectively. In the ABTS assay, nanodispersions produced weaker results than their free counterparts, where 1 μM of effective Nano-Lut concentration was equivalent to $1.735 \pm 0.099 \mu\text{M}$ of Trolox, **Figure 5 A**.

In contrast, FRAP and iron metal chelation assays indicated that the nanodispersion system enhanced the antioxidant capacity of the free molecules. The results showed that 1 μM EBc (effective concentration) was equivalent to $0.713 \pm 0.011 \mu\text{M}$ Trolox standard in FRAP assay and $0.417 \pm 0.04 \mu\text{M}$ EDTA in iron chelation assay while, in Nano-EBc, it was significantly higher and was equivalent to $1.463 \pm 0.114 \mu\text{M}$ Trolox and $0.662 \mu\text{M}$ EDTA, respectively. (**Figure 5B and 5C**).

The same was applied in the DPPH where the IC₅₀ values of the tested free carotenoids were lower than their nanodispersions where the IC₅₀ achieved by Lut is 3.453 μ M compared to Trolox positive control in methanol which achieved 16.45 \pm 1.25 μ M IC₅₀ value. While the IC₅₀ value of the Nano-Lut was significantly higher reaching 23.22 \pm 1.68 μ M compared to Trolox positive control in water which achieved an IC₅₀ value of 41.95 \pm 8.5 μ M IC₅₀ value as depicted in **Figure 6**.

Table 3: Results of free and nanodispersion carotenoids using different antioxidant assays.

Free/ carotenoid nanodispersions	Antioxidant Assay				
	DPPH (IC ₅₀ μ M)	ABTS (μ M T Eq/ μ M)	FRAP (μ M T Eq/ μ M)	Iron chelation (μ M EDTA Eq/ μ M)	ORAC (μ M T Eq/ μ M)
Lut	3.453 \pm 0.526 ^a	4.546 \pm 0.320 ^a	0.882 \pm 0.019 ^a	0.439 \pm 0.039 ^a	26.507 \pm 2.112
EBc	9.417 \pm 0.73 ^{a, b}	4.066 \pm 0.280 ^a	0.714 \pm 0.011 ^a	0.417 \pm 0.04 ^{a, b}	1.021 \pm 0.078 ^a
SBc	10.28 \pm 1.39 ^{a, b}	1.860 \pm 0.109 ^b	0.342 \pm 0.032	0.271 \pm 0.007 ^b	0.662 \pm 0.056 ^a
Nano-Lut	23.22 \pm 1.68 ^b	1.735 \pm 0.099 ^b	1.766 \pm 0.058 ^b	0.743 \pm 0.079 ^c	N/A
Nano-EBc	56.78 \pm 9.68	1.284 \pm 0.098 ^{b, c}	1.463 \pm 0.113 ^{b, c}	0.629 \pm 0.036 ^{c, d}	N/A
Nano-SBc	98.12 \pm 11.56	0.982 \pm 0.017 ^c	1.191 \pm 0.022 ^c	0.591 \pm 0.017 ^d	N/A

DPPH is expressed as IC₅₀ while FRAP, ABTS, and ORAC are expressed as μ M Trolox equivalent/ μ M carotenoid and Iron chelation results are expressed as μ M EDTA equivalent / μ M carotenoid. Data labeled with the same letter in each column (antioxidant test type) denote non-significant differences and different letters denote significant differences at P < 0.05.

Additionally, the ORAC assay exhibited the same pattern, with 1 μ M Lut effective concentration being equivalent to 26.5 μ M Trolox in the postponement of fluorescein's oxidative degradation (**Figure 7 and Table 3**). However, this assay was affected by the ingredients of the nano-system vehicle where tween 80 in

water at different concentrations produced a significant activity that could mask the effect of the tested molecules (data not shown).

Cell culture and cytotoxicity assay

Cytotoxicity of free and nanodispersion of Lut, EBc, and SBc at different concentrations was assessed on normal human skin, green monkey kidney, and mice liver cell lines. The cytotoxic activity was investigated by the survival fraction percent by using an SRB assay. Lut did not potentially display cytotoxicity on the tested cell lines as shown in **Table 4**, however, when fabricated into nanodispersion, it showed increased cytotoxic activity with the different cell lines used. The highest used effective concentration of Lut (100 µg/ml) showed 70.52±0.92, 52.1±0.49, and 94.73±3.72 cell viability percentages (IC₅₀) with HSF, VERO, and BNL, respectively. Based on the above results and depending on the normal cell type, free lutein showed the lowest cytotoxic efficacy against HSF, VERO, and BNL lines **Table 4**.

EBc or its nanodispersion form was assessed against the same cell lines, and the cytotoxic activity was investigated. The IC₅₀ values with HSF-treated cells were 35.76 ± 5.56, and 51.52 ± 4.99 µg/ml for EBc, and Nano-EBc, respectively. In VERO and BNL-treated cells, the IC₅₀ of Nano-EBc was decreased insignificantly (P>0.05) from 17.91 ± 3.80 and 34.57 ± 1.84 to 10.66 ± 1.24 and 27.8 ± 1.85 µg/ml, respectively when compared to EBc.

When Nano-SBc was administered with HSF and BNL-treated cells, the IC₅₀ showed increased cytotoxicity when compared to SBc. The IC₅₀ was insignificantly changed from 24.54 ± 3.67 and 22.04 ± 1.71 to 25.92 ± 5.58 and 27.91 ± 1.10 µg/ml with HSF and BNL, respectively. In VERO-treated cells, the cytotoxicity was decreased by the administration of Nano-SBc as IC₅₀ was changed from 18.11 ± 1.87 to 6.57 ± 0.32 µg/ml.

0.1% Tween 80 did not potentially influence the cytotoxicity for all tested cell lines as shown in **Table 4**, however, 1% Tween 80 showed increased cytotoxicity against HSF and VERO cell lines. 0.1% Tween 80 with an equivalent volume of the highest lutein concentration (100 µg/ml) showed 95.01±1.33, 89.39±3.04, and 102.108±0.11 cell viability percentage with HSF, VERO, and BNL, respectively. Interestingly, BNL cells showed tolerance for 1% Tween 80 as the equivalent volume of the highest concentration (100 µg/ml) showed a 100.99±3.72 cell viability ratio.

Table 4: Cytotoxicity results of free and nanodispersion carotenoids on 3 different normal cell lines.

	HSF	VERO	BNL
0.1% Tween 80	>100*	>100*	>100*
1% Tween 80	65.56 ± 1.10 ^a	28.107 ± 3.25 ^a	>100*
Lut	>100*	>100*	>100*
SBc	24.54 ± 3.67 ^b	18.11 ± 1.87 ^{a, b}	22.04 ± 1.71 ^a
EBc	35.76 ± 5.56 ^b	17.91 ± 3.80 ^{a, b}	34.57 ± 1.84 ^a
Nano-Lut	59.16 ± 6.16 ^a	21.67 ± 3.61 ^a	30.99 ± 3.40 ^a
Nano-SBc	25.92 ± 5.58 ^b	6.57 ± 0.32 ^b	27.91 ± 1.10 ^a
Nano-EBc	51.52 ± 4.99 ^a	± 1.124 ^b	27.8 ± 1.85 ^a

Cytotoxicity IC₅₀ was expressed as effective concentration (µg/ml). Data labeled with the same letter in each column (each cell line) denote non-significant differences and different letters denote significant differences at P < 0.05. * Donates the IC₅₀ was more than 100 µg/ml (safe treatment).

Discussion

presented in this study conditions to formulate carotenoids in nanodispersions using Tween 80 as an available surfactant and examined their physicochemical, antioxidant, and cytotoxic properties compared with their free forms. Nano-Lut and Nano-SBc showed narrow particle distribution, as reflected in PDI (**Table 2**), and monomodal peaks [**Figure 3 (A and B)**]. The fabricated Nano-EBc showed an increase in the mean size diameter in comparison with Nano-SBc, however, Nano-EBc showed a bimodal distribution. The bimodal distribution of Nano-EBc might be due to their mixed structure of all-trans and cis isomers however, this was not displayed by SBc because it consisted of all-trans isomers only. The narrow particle size distributions represented by the PDI values observed from this study bode well for the homogeneity of nanodispersions [40].

Ostwald ripening process is widely recognized as the main mechanism causing the instability of nanodispersions. The narrow particle distribution would mean that the nanodispersions are less susceptible to the Ostwald ripening process. Due to the expansion of large particles at the expense of small particles, this phenomenon causes the average particle size to increase. In this respect, it can be claimed that the Ostwald ripening phenomena is more evident in systems

with a wide range of particle sizes [41, 42]. Thus, in the present study, we expect Nano-Lut and Nano-SBc to be physically stable due to their observed PDI.

zeta potential's magnitude indicates the potential stability of colloidal systems. As the zeta potential increases, repulsion between particles will be greater, leading to a more stable colloidal dispersion. If all particles in suspension have a large negative or positive zeta potential, then they will tend to repel each other and there will be no tendency for the particles to aggregate [42]. In a nanodispersion system, the zeta potential of a particle can be used as an indicator of long-term physical stability. The results of zeta potential measurements of the produced nanodispersions were -28.6 ± 6.4 , -12.1 ± 5.9 , and -39.7 ± 1.3 for Nano-Lut, Nano-SBc, and Nano-EBc, respectively. These zeta potential values indicate that the prepared nanodispersions have good physical stability.

loss of all the nanodispersions during the preparation in the present study was <20% (Table 2). The final content of Nano-Lut and Nano-SBc were not significantly ($p < 0.05$) different from each other (Table 2). This finding also indicates that the solvent displacement is a suitable method for preparing sensitive compounds nanodispersions, as the final nanodispersions contents shown were promising (>80%).

size, PDI, zeta potential, and drug content of Nano-Lut were similar to the previously reported lutein nanodispersions using 0.1% T80 prepared with the solvent displacement method. Tan et al. [25,26] added the organic phase dropwise to the aqueous phase to prepare lutein nanodispersion in the same manner as the present work. This nanodispersion had a smaller particle size (≈ 75 nm), however, a higher PDI (0.22), a lower drug content (<85%), and a lower zeta potential (-7.73 ± 0.01 mV) in comparison to the results of the present study. In another study [27], it was reported that the particle size and PDI were 123.1 ± 0.3 nm, and 0.155 ± 0.008 , respectively with drug content (93.16%) after applying a similar preparation procedure used in this study. Adding the organic phase to the aqueous phase dropwise produces a smaller particle size with higher PDI in comparison to one-shot addition. This concept was studied for lutein nanodispersions where the particle size and PDI were reported to be 70-80 nm and 0.18-0.2, respectively, when the addition was dropwise and was 120-140 nm and 0.14-0.16 when added in a one-shot manner [28].

pared to the available literature, Bc nanodispersion was generated in the present study with improved properties. Anarjan et al. [15] using a similar method have generated Bc nanodispersion by using acetone as the organic phase rather than n-hexane and homogenized the mixture rather than stirring it with a magnetic stirrer. It was found that the particle size was smaller (136.7 nm) however, the loss in Bc was significantly higher (59.4%). Bc (0.015% w/v) and tween 20 (1%) were used to prepare nanodispersion with acetone as the organic phase, the particle size was smaller, however, the distribution was bimodal, and the zeta potential was -8.2 mV [31]. This can be explained by the fact that Bc is more soluble in n-hexane than acetone which leads to better distribution and homogeneity, moreover, the higher stability in our results could be attributed to the fact that the homogenizer produces high energy that could harm heat-sensitive compounds as Bc.

UV-Vis spectra of the Lut, SBc, and EBc in comparison with their nanodispersions were evaluated in the present study. The pronounced hypsochromic spectral shift in the Nano-Lut was an indication of the strong excitonic coupling owing to the close localization of adjacent polyene chains. The Lut-Nano was much more absorptive in the UVA region of the electromagnetic spectrum, meaning lutein converted to an H-aggregation structure [43, 44]. The spectral shifts observed in Nano-SBc and Nano-EBc (bathochromic shift) could be interpreted in terms of the formation of different coupled structures however, SBc (which consists of all trans isomers only) was more incorporated in the nanodispersion system than EBc (which consists of many isomers) [44, 45].

analysis in the present study revealed potent antioxidant effects in all the assays for both free and nanodispersion of carotenoids. Indeed, their chemical structure, which includes a long conjugation of double bonds allows them to quench and stabilize free radicals [6, 46]. This explains their activity towards DPPH and ABTS assays which involve the reaction directly with the free radicals. In DPPH and ABTS assays, the free radicals have distinguished colors that fade away in the presence of a potent antioxidant. This decrease can be determined by simple colorimetric approaches [47]. Moreover, the ORAC assay involves the in-situ production of peroxy free radicals that can degrade fluorescein by oxidation. Therefore, the presence of an antioxidant can delay this process (Figure 7). It can be suggested that their chemical structure also allows them to exert antioxidant effects via electron transfer mechanism in addition to proton transfer. This is concluded from the results of the FRAP assay that involves a redox reaction to convert the Fe^{+3} -TPTZ complex into Fe^{+2} -TPTZ complex [48]. Furthermore, the results indicated another important activity as metal chelators indicated by ferrozine iron metal chelation assay that relies on the converting principle of Fe^{+2} , which can transfer single electrons and form free radicals, into Fe^{+3} [49, 50]. Hence, it may be concluded that carotenoids exert their antioxidant activity by different mechanisms.

observed that Lut was the most potent antioxidant among the tested carotenoids. In comparison to the data in the literature, Jimenez-Escrig et al. [51] contradict this result and found that Bc has an IC_{50} value in DPPH assay of 2.26 ± 0.09 mole/mole DPPH while that of lutein is 3.29 ± 0.31 mole/mole DPPH. However, the authors in this assay recorded the absorbance after adding the DPPH solution at 580 nm without subtracting the compound color. This was explained by the notion that the inherent interference of the compounds was neglected at this wavelength, which was far from the maximum absorbance achieved by the DPPH free radical. In our experiment, to minimize the interference of the carotenoids' original color, we used small concentrations and subtracted the resulting readings from blank samples containing the carotenoids without DPPH solution at 517 nm.

our knowledge, the studies on carotenoid antioxidant activity used the actual weight of the component, leading to variations from one study to another. Carotenoids are sensitive components, they can easily degrade during storage or use, so the actual weight may lead to misleading results. For this reason, we used the concentrations expressed as molar effective concentrations rather than the conventional molar concentrations. This could also explain the alteration in the order of potency reported by Tan, et al. [52] who used the mg/mL

concentration. However, this study confirmed that when the carotenoids are in liposomes, they follow the same pattern of potency reported by our study regarding Lut and Bc.

cova, et al. [53] used the ABTS free radical assay to evaluate different antioxidant compounds, including Lut and Bc. They found a slight difference in the activity of these two carotenoids, with 100 µg/mL of lutein equivalent to just over 60 µg/mL of Trolox and Bc equivalent to about 70 µg/mL of Trolox. This measurement was assessed after only 5 minutes of incubation, which may not have been enough to exert the effect because some plant-derived metabolites may exhibit complex kinetic interactions with ABTS cation. This study also used the weight per volume expression of concentration [54].

Considering the ORAC assay, our findings were similar to those obtained by Zulueta et al. [55] where the activity of Lut was twice that of Bc. However, we evaluated the carotenoids in comparison to the fluorescein with the same excitation and emission wavelengths used in the ORAC to assess compounds' intrinsic fluorescence according to the significant difference between the activity of lutein and the standard Trolox and β-carotene in our results, and we found that there was no significant intrinsic fluorescence detected. This indicates that the ORAC assay might be a convenient assay to assess the carotenoids' antioxidant capacity, however, it was unreliable to assess their nanodispersion due to vehicle interference.

Interestingly, it was observed that the carotenoid nanodispersions are less reactive than their free compounds in DPPH and ABTS assays and more reactive towards FRAP and ferrozine (Table 3). Although it is well-reported that advanced drug delivery systems enhance the bioavailability of carotenoids and hence their activity [56], DPPH and ABTS are in-vitro cell-free assays where the reagents are dissolved in methanol, and their interaction with the tested samples or formulas is purely chemically based. Therefore, the decrease in activity towards these assays may be explained due to the interference of the solvent and/or the T80 in the formula with the reaction. Indeed, being lipophilic compounds, carotenoids prefer organic solvents to water to dissolve in [23], and the presence of alcohol in ABTS and DPPH assay as a solvent for the free radicals might encourage the reaction with the free carotenoid. It is distributed fairly in the medium of the reaction while it might disrupt the distribution of molecules between the nano-system and the reaction media preventing some molecules from the reaction.

In contrast with FRAP and iron metal chelation assays, the reagents in these two assays were dissolved in aqueous media, this allowed better distribution of the nanodispersion particles in the medium of the reaction than the distribution of the free molecules that aggregated in water. Hence, in the case of FRAP and metal chelation assays, nanodispersion reduces the tension in the reaction medium while disturbing the distribution of molecules in the case of the free radical-scavenging assay (DPPH and ABTS).

It is worth mentioning that the results of DPPH and FRAP contradict some previous reports where the formulated carotenoids exerted better results. As previously mentioned, the results of Tan et al. [52] reported an increase in the activity toward DPPH and FRAP assays when the carotenoids were in liposomes. However, each drug delivery system has distinctive characteristics.

rding the ORAC assay, although it followed the same order of potency as the other investigated assays, the formulated compound interfered with the results where the vehicle of the formulas (Tween 80 with the same ratios and deionized water) masked the results and delayed the oxidative degradation of fluorescein with unreproducible results in independent trials. For this reason, we excluded this assay in the comparison of the tested nanodispersions.

n the activities of the EBc and SBc were compared, EBc showed greater potency as an antioxidant agent. This can be explained by the notion that different isomers exert a synergistic effect; each isomer reacts with the target in different potencies that altogether adds up to the final activity, as documented in earlier studies [57-62]. To our knowledge, studies that compared the EBc and SBc in terms of in-vitro cell-free antioxidant assays or even in vivo studies were scarce. Liu et al. [63] found the potential and equal activity of the all-trans isomers of SBc and the natural 9-cis β -carotene isomer using enhanced human neutrophil chemiluminescence. An earlier study concluded that the natural 9-cis isomer is a more potent antioxidant than all-trans isomers of SBc [64]. This was concluded by the reduced amount of serum oxidized digenic products of human subjects supplemented with natural 9-cis β -carotene isomer compared to others supplemented with all-trans isomers of SBc. On the other hand, Lavy et al. [65] found that although Bc in the two forms can bind efficiently to low-density lipoprotein (LDL), the synthetic one is two folds more active than the natural counterpart in terms of LDL lipid peroxidation.

efore, the antioxidant effect of the isomers should be more readily investigated in terms of in-vivo and in-vitro approaches. The mentioned studies used the actual weight/concentration and compared only the all-trans isomers of SBc with 9-cis natural Bc, which led to a misleading comparison because the natural sources of Bc differ in their effective amount and contain many Bc isomers not only 9-cis isomer. In the present study, EBc from carrots contains the two mentioned isomers; all trans and 9-cis isomers, in addition to the 13-cis isomer (detailed in the supplementary data). It could be concluded that the natural mixture provides a higher activity compared with SBc. Additionally, all performed assays showed that EBc has greater antioxidant activity than SBc. This was also found when these three ingredients were formulated as the nanodispersion system; Nano-Lut remained more potent than Nano-EBc and Nano-SBc.

result showed that Lut was less cytotoxic against HSF, VERO, and BNL cell lines, (IC_{50} more than 100 μ g/ml), it was significantly ($P<0.05$) safer than Bc from the two sources and this might be due to Bc can turn from an antioxidant agent to a prooxidant agent [66-69].

all the investigated cell lines, the cell tolerance did not substantially differ between SBc and EBc. A similar observation was made for the Nano-SBc and Nano-EBc with VERO and BNL. However, there was a significant ($P<0.05$) difference against HSF, where Nano-SBc was twice as toxic as Nano-EBc. The IC_{50} value of Bc was not significantly ($P<0.05$) affected after forming the nanodispersion in all tested cell lines except in the case of EBc and Nano-EBc against HSF. Nano-Lut was significantly more cytotoxic than its free form with HSF, VERO, and BNL. The variation in IC_{50} values for each cell line was anticipated as each species' and organ's tolerance varies depending on biocompatibility and the requirement for carotenoids [70, 71].

he best of our knowledge, the cytotoxicity of carotenoid nanodispersions was not yet studied against normal cell lines to investigate the safety of their use. However, the safety of Lut, SBc, and EBc was assessed against some normal cell lines.

normal breast cell lines, MCF-10A exhibited 95% viability after 48 hours when treated with a range of concentrations up to 100µg/mL lutein extracted from Calendula flowers [72]. Equivalent results against the same cell line were obtained in another study with lutein and β-carotene extracted from spinach with a dose of 20 µM and an incubation period of 72 hours [73]. Moreover, another study confirmed the safety of lutein and β-carotene against primary mammary epithelial cell line (PmECs) at a low range of concentration up to 2µM for 48 hours [74]. However, the characteristics of the tested carotenoid in terms of purity or stereochemistry were not examined, no toxicity was observed on the normal colon cell line (CCD 841 CoTr) when treated with lutein extracted from spinach at a dose of up to 10µM for 48 hours [75]. The same pattern was observed with the human bronchial epithelial cell line (BEAS-2B) when these cells were treated with Lut or Bc for 48 h with a narrow range of concentrations (0, 0.5, 1, and 2 µM) [76]. Furthermore, free and chitosan alginate polymeric nanoparticles of lutein (particle size of 98±5 nm and zeta potential of 38±4 mV) extracted from marigold petals were evaluated on human retinal pigment epithelial (ARPE-19) cell line at a dose up to 50µM for 24 hours [77]. Accordingly, it can be concluded that carotenoids exert a selective toxic effect on cancer cell lines and high safety profiles to normal cells [72-77].

Conclusion

The current study focused on the formulation of Lut, EBc, and SBc nanodispersions using the solvent displacement method in comparison with their free forms. Furthermore, it examined the distinction between carotenoids extracted from natural sources and those from synthesized sources. The solvent displacement technique was effectively used to produce Nano-Lut, Nano-EBc, and Nano-SBc and showed an effective performance of carotenoids in an aqueous medium owing to Tween 80. Our study in comparison with earlier studies emphasized the importance of quantizing carotenoids as an effective weight/ concentration. As carotenoids are active and sensitive antioxidants, the use of actual weight/ concentration only does not reflect their actual activity, leading to an enormous difference between one source and another. Our research showed that Lut and Bc properties are influenced by a variety of variables, including the source (extracted or synthetic), the environment (the level of free radicals, type of cells, etc.), and the used isomer(s). As noticed, most of the previous literature used actual weight/concentration while in our study we used the effective concentrations, and both proved the safety on the most normal cell lines. The cytotoxicity assay was conducted in a completely stress-free optimal environment. We may infer from the cytotoxicity assay results and the antioxidant activities that carotenoids need to be studied more thoroughly under various situations to understand their chemical and physical stabilities in their different applications.

Declarations

Author's Contribution

Nourhan S. Elkholy: Suggested the idea, analyzed and interpreted the extraction, purification, and identification of carotenoids, prepared and characterized the nanodispersions, and contributed to data curation, writing, editing, and visualization.

Mohamed Louai M. Hariri: contributed to the extraction, purification, and identification of carotenoids, performed and interpreted antioxidant activities, and contributed to data curation, writing, editing, and visualization.

Haitham S. Mohammed: Conceptualized the work, supervised the workflow, and contributed to data curation, writing, review, and editing.

Medhat W. Shafaa: was a major contributor to writing the manuscript, validated the methodology, supervised the workflow, and contributed to data curation.

All authors read and approved the final manuscript.

The authors have no relevant financial or non-financial interests to disclose.

The authors have no conflicts of interest to declare relevant to this article's content.

All authors certify that they have no affiliations with or involvement in any organization or entity with any financial interest or non-financial interest in the subject matter or materials discussed in this manuscript.

The authors have no financial or proprietary interests in any material discussed in this article.

No funding was obtained for this study

References

1. G. Sandmann, Trends Plant Sci. 6(1), 14-17 (2001). [https://doi.org/10.1016/s1360-1385\(00\)01817-3](https://doi.org/10.1016/s1360-1385(00)01817-3)
2. A. G. Murillo, M. L. Fernandez, Adv. Nutr. 7(1), 14-24 (2016). <https://doi.org/10.3945/an.115.009803>
3. M. Eggersdorfer, A. Wyss, Arch. Biochem. Biophys. 652, 18-26 (2018).
<https://doi.org/10.1016/j.abb.2018.06.001>
4. M. L. Failla, T. Huo, S. K. Thakkar, Asia Pac J Clin Nutr. 17(Suppl 1), 200-3 (2008).
5. A. R. Collins, Mutat. Res. Fundam. Mol. Mech. Mutagen. 475(1-2), 21-28 (2001).
[https://doi.org/10.1016/S0027-5107\(01\)00071-9](https://doi.org/10.1016/S0027-5107(01)00071-9)
6. S. Maghsoudi, B. Taghavi Shahraki, N. Rabiee, Y. Fatahi, M. Bagherzadeh, R. Dinarvand, T. J. Webster, Crit. Rev. Food Sci. Nutr. 62(13), 3658-3697 (2022).
<https://doi.org/10.1080/10408398.2020.1867958>
7. P. Mapelli-Brahm, F. J. Barba, F. Remize, C. Garcia, A. Fessard, A. M. Khaneghah, A.J. Meléndez-Martínez, Trends Food Sci. Technol. 99, 389-401 (2020). <https://doi.org/10.1016/j.tifs.2020.03.013>

8. H. Van den Berg, R. Faulks, H. F. Granado, J. Hirschberg, B. Olmedilla, G. Sandmann, W. Stahl, J. Sci. Food Agric. 80(7), 880-912 (2000). [https://doi.org/10.1002/\(SICI\)1097-0010\(20000515\)80:7<880::AID-JSFA646>3.0.CO;2-1](https://doi.org/10.1002/(SICI)1097-0010(20000515)80:7<880::AID-JSFA646>3.0.CO;2-1)
9. D. A. Cooper, J. Nutr. 134(1), 221S-224S (2004). <https://doi.org/10.1093/jn/134.1.221S>
10. D. B. Rodriguez-Amaya, A guide to carotenoid analysis in foods (Vol. 71). (Washington: ILSI press 2001).
11. C. I. Cazzonelli, N. Nisar, D. Hussain, M. E. Carmody, B. J. Pogson, Biosynthesis and Regulation of Carotenoids in Plants—micronutrients, vitamins, and health benefits. (Springer, Berlin, Heidelberg 2010), pp. 117-137
12. R. Cooper, G. Nicola, Natural products chemistry: sources, separations and structures. (CRC press 2014).
13. Z. Wang, M. A. Neves, H. Isoda, M. Nakajima, Jpn. J. Food Eng. 16(4), 263-276 (2015). <https://doi.org/10.11301/jsfe.16.263>
14. P. N. Ezhilarasi, P. Karthik, N. Chhanwal, C. Anandharamakrishnan, Food Bioprocess Technol. 6(3), 628-647 (2013). <https://doi.org/10.1007/s11947-012-0944-0>
15. N. Anarjan, M. Fahimdanesh, H. Jafarizadeh-Malmiri, J. Food Sci. Technol. 54(11), 3731-3736 (2017). <https://doi.org/10.1007/s13197-017-2764-8>
16. Y. J. Park, S. Y. Park, M. Valan Arasu, N. A. Al-Dhabi, H. G. Ahn, J. K. Kim, S.U. Park, Mol. 22(2), 313 (2017). <https://doi.org/10.3390/molecules22020313>
17. D. B. Rodrigues, A. Z. Mercadante, L. R. B. Mariutti, Food Res. Int. 119, 653-664 (2019). <https://doi.org/10.1016/j.foodres.2018.10.043>
18. F. Khachik, A. Steck, H. Pfander, J. Agric. Food. Chem. 47(2), 455-461 (1999). <https://doi.org/10.1021/jf980823w>
19. P. Gupta, Nat Prod Chem Res, 2(6), e110 (2014). <http://dx.doi.org/10.4172/2329-6836.1000e110>
20. E. Rahayuningsih, D. A. Wikansari, H. Setiawan, ASEAN J. Chem. Eng. 16(2), 44-58 (2016).
21. R. M. Al-Ali, S. A. Al-Hilifi, A. E. H. J. Al-Mossawi, Plant Arch. 20(1), 1679-1685 (2020).
22. P. Boonnoun, T. Opaskonkun, P. Prasitchoke, M. Goto, A. Shotipruk, Eng. J. 16(5), 145-156 (2012). <https://doi.org/10.4186/ej.2012.16.5.145>
23. N. E. Craft, J. H. Soares, J. Agric. Food. Chem. 40(3), 431-434 (1992). <https://doi.org/10.1021/jf00015a013>
24. M. Rifqi, I. S. Setiasih, Y. Cahayana, In IOP Conference Series: Earth and Environmental Science (Vol. 443, No. 1, p. 012063) (2020, February). <https://doi.org/10.1088/1755-1315/443/1/012063>
25. T. B. Tan, N. S. Yussof, F. Abas, H. Mirhosseini, I. A. Nehdi, C. P. Tan, Food Chem. 205, 155-162 (2016). <https://doi.org/10.1016/j.foodchem.2016.03.008>
26. T. B. Tan, W. C. Chu, N. S. Yussof, F. Abas, H. Mirhosseini, Y. K. Cheah, C. P. Tan, Food Funct. 7(4), 2043-2051 (2016). <https://doi.org/10.1039/C5FO01621E>

27. T. B. Tan, N. S. Yussof, F. Abas, H. Mirhosseini, I. A. Nehdi, C. P. Tan, J. Food Eng. 177, 65-71 (2016).
<https://doi.org/10.1016/j.jfoodeng.2015.12.020>
28. T. B. Tan, N. S. Yussof, F. Abas, H. Mirhosseini, I. A. Nehdi, C. P. Tan, Food Chem. 194, 416-423 (2016).
<https://doi.org/10.1016/j.jfoodeng.2015.12.020>
29. C. P. Tan, M. Nakajima, Food Chem. 92(4), 661-671 (2005).
<https://doi.org/10.1016/j.foodchem.2004.08.044>
30. H. S. Ribeiro, B. S. Chu, S. Ichikawa, M. Nakajima, Food Hydrocolloids, 22(1), 12-17 (2008).
<https://doi.org/10.1016/j.foodhyd.2007.04.009>
31. L. J. Yin, B. S. Chu, I. Kobayashi, M. Nakajima, Food Hydrocolloids 23(6), 1617-1622 (2009).
<https://doi.org/10.1016/j.foodhyd.2008.12.005>
32. M. B. Arnao, A. Cano, M. Acosta, Food Chem. 73(2), 239-244 (2001). [https://doi.org/10.1016/S0308-8146\(00\)00324-1](https://doi.org/10.1016/S0308-8146(00)00324-1)
33. I. F. Benzie, J. J. Strain, Anal. Biochem. 239(1), 70-76 (1996). <https://doi.org/10.1006/abio.1996.0292>
34. J. S. Santos, V. R. A. Brizola, D. Granato, Food Chem. 214, 515-522 (2017).
<https://doi.org/10.1016/j.foodchem.2016.07.091>
35. R. Boly, T. Lamkami, M. Lompo, J. Dubois, I. Guissou, Int. J. of Toxicol. Pharmacol. Res. 8(1), 29-34 (2016).
36. Z. Chen, R. Bertin, G. Foldi, Food Chem. 138(1), 414-420 (2013).
<https://doi.org/10.1016/j.foodchem.2012.11.001>
37. Z. Liang, L. G. Y. Cheng, Zhong, R.H. Liu, PloS one, 9(8), e105146 (2014).
<https://doi.org/10.1371/journal.pone.0105146>
38. P. Skehan, R. Storeng, D. Scudiero, A. Monks, J. McMahon, D. Vistica, J. T. Warren, H. Bokesch, S. Kenney, M. R. Boyd. J. Natl. Cancer Inst. 82(13): 1107-1112 (1990). <https://doi.org/10.1093/jnci/82.13.1107>
39. R. M. Allam, A. M. Al-Abd, A. Khedr, O. A. Sharaf, S. M. Nofal, A. E. Khalifa, A. B. Abdel-Naim, Toxicol. Lett. 291, 77-85 (2018). <https://doi.org/10.1016/j.toxlet.2018.04.008>
40. A. Forgiarini, J. Esquena, C. Gonzalez, C. Solans, *Langmuir*, 17(7), 2076-2083 (2001).
<https://doi.org/10.1021/la001362n>
41. T. Tadros, P. Izquierdo, J. Esquena, C. Solans, Adv. Colloid Interface Sci. 108, 303-318 (2004).
<https://doi.org/10.1016/j.cis.2003.10.023>
42. Y. Liu, K. Kathan, W. Saad, R. K. Prud'homme, Phys. Rev. Lett. 98(3), 036102 (2007).
<https://doi.org/10.1103/PhysRevLett.98.036102>
43. G. Britton, The FASEB J. 9(15), 1551-1558 (1995). <https://doi.org/10.1096/fasebj.9.15.8529834>
44. N. E. Polyakov, A. Magyar, L. D. Kispert, J. Phys. Chem. B, 117(35), 10173-10182 (2013).
<https://doi.org/10.1021/jp4062708>
45. L. Cao-Hoang, R. Fougère, Y. Waché, Food Chem. 124(1), 42-49 (2011).
<https://doi.org/10.1016/j.foodchem.2010.05.100>

46. A. J. Young, G. L. Lowe, *Antioxid.* 7(2), 28 (2018). <https://doi.org/10.3390/antiox7020028>
47. I. G. Munteanu, C. Apetrei, *Int. J. Mol. Sci.* 22(7), 3380 (2021). <https://doi.org/10.3390/ijms22073380>
48. L. Cerretani, A. Bendini, *Olives Olive Oil Health Dis. Prev.* 625-635, Academic Press (2010).
<https://doi.org/10.1016/B978-0-12-374420-3.00067-X>
49. J. P. Adjimani, P. Asare, *Toxicol. Rep.* 2, 721-728 (2015). <https://doi.org/10.1016/j.toxrep.2015.04.005>
50. A. M. Aboul-Enein, F. K. El Baz, G. S. El-Baroty, A. M. Youssef, H. H. Abd El-Baky, *Asian Network Sci. Inf.* (2003).
51. A. Jiménez-Escrig, I. Jiménez-Jiménez, C. Sánchez-Moreno, F. Saura-Calixto, *J. Sci. Food Agric.* 80(11), 1686-1690 (2000). [https://doi.org/10.1002/1097-0010\(20000901\)80:11<1686::AID-JSFA694>3.0.CO;2-Y](https://doi.org/10.1002/1097-0010(20000901)80:11<1686::AID-JSFA694>3.0.CO;2-Y)
52. C. Tan, J. Xue, S. Abbas, B. Feng, X. Zhang, S. Xia, *J. Agric. Food. Chem.* 62(28), 6726-6735 (2014).
<https://doi.org/10.1021/jf405622f>
53. Z. Kotíková, J. Lachman, A. Hejtmánková, K. Hejtmánková, *LWT Food Sci. Technol.* 44(8), 1703-1710 (2011). <https://doi.org/10.1016/j.lwt.2011.03.015>
54. M. Ozgen, R. N. Reese, A.Z. Tulio, J.C. Scheerens, A. R. Miller, *J. Agric. Food. Chem.* 54(4), 1151-1157 (2006). <https://doi.org/10.1021/jf051960d>
55. A. Zulueta, M. J. Esteve, A. Frígola, *Food Chem.* 114(1), 310-316 (2009).
<https://doi.org/10.1016/j.foodchem.2008.09.033>
56. H. Rostamabadi, S. R. Falsafi, S. M. Jafari, *J. Controlled Release* . 298, 38-67 (2019).
<https://doi.org/10.1016/j.jconrel.2019.02.005>
57. A. Ben-Amotz, Y. Levy, *Am. J. Clin. Nutr.* 63(5), 729-734 (1996).
<https://doi.org/10.1016/j.jconrel.2019.02.005>
58. J. J. Challem, *J. Nat. Cancer Inst.* 89(4), 325-325 (1997). <http://10.1093/jnci/88.21.1550>
59. J. J. Challem, *J. Orthomol. Med.* 12(1), 11-19 (1997).
60. Xue, K. X., Wu, J. Z., Ma, G. J., Yuan, S., & Qin, H. L. *Mutation Research/Genetic Toxicology and Environmental Mutagenesis*, 418(2-3), 73-78 (1998). [https://doi.org/10.1016/S1383-5718\(98\)00109-0](https://doi.org/10.1016/S1383-5718(98)00109-0)
61. Ghazi, A. (1999). *Food Nahr.* 43(4), 274-277. [https://doi.org/10.1002/\(SICI\)1521-3803\(19990801\)43:4<274::AID-FOOD274>3.0.CO;2-S](https://doi.org/10.1002/(SICI)1521-3803(19990801)43:4<274::AID-FOOD274>3.0.CO;2-S)
62. EFSA Panel on Food Additives and Nutrient Sources added to Food (ANS), *EFSA J.*, 10(3), 2593 (2012).
<https://doi.org/10.2903/j.efsa.2012.2593>
63. Q. Liu, K. Suzuki, S. Nakaji, K. Sugawara, *Nutr. Res.* 20(1), 5-14 (2000). [https://doi.org/10.1016/S0271-5317\(99\)00133-5](https://doi.org/10.1016/S0271-5317(99)00133-5)
64. A. Ben-Amotz, Y. Levy, *Am. J. Clin. Nutr.* 63(5), 729-734 (1996). <https://doi.org/10.1093/ajcn/63.5.729>
65. A. Lavy, A. Ben Amotz, M. Aviram, *Biochem. Vol* 31, pp. 83-90 (1993).
<https://doi.org/10.1515/cclm.1993.31.2.83>
66. P. Palozza, S. Serini, F. Di Nicuolo, E. Piccioni, G. Calviello, *Mol. Aspects Med.* 24(6), 353-362 (2003).
[https://doi.org/10.1016/S0098-2997\(03\)00031-1](https://doi.org/10.1016/S0098-2997(03)00031-1)

67. S. Kawanishi, S. Oikawa, M. Murata, *Antioxid. Redox Signaling*. 7(11-12), 1728-1739 (2005).
<https://doi.org/10.1089/ars.2005.7.1728>
68. P. Palozza, *Biochim. Biophys. Acta, Mol. Basis Dis*, 1740(2), 215-221 (2005).
<https://doi.org/10.1016/j.bbadis.2004.12.008>
69. X. Gong, J. R Smith, H. M. Swanson, L. P. Rubin, *Mol.* 23(4), 905 (2018).
<https://doi.org/10.3390/molecules23040905>
70. V. Shete, L. Quadro, *Nutr.* 5(12), 4849-4868 (2013). <https://doi.org/10.3390/nu5124849>
71. A. S. Green, A. J. Fascetti, *Sci. World J.* (2016). <https://doi.org/10.1155/2016/7393620>
72. M. Behbahani, *PloS one*, 9(12), e116049 (2014). <https://doi.org/10.1371/journal.pone.0116049>
73. P. R. R. Sowmya, B. P. Arathi, K. Vijay, V. Baskaran, R. Lakshminarayana, *Food Chem. Toxicol.* 106, 58-69 (2017). <https://doi.org/10.1016/j.fct.2017.05.024>
74. J. L Schwartz, J. Tanaka, V. Khandekar, T. S. Herman, B. A. Teicher, *Cancer Chemother. Pharmacol.* 29(3), 207-213 (1992). <https://doi.org/10.1007/BF00686254>
75. W. Grudzinski, M. Piet, R. Luchowski, E. Reszczynska, R. Welc, R. Paduch, W.I. Gruszecki, *Spectrochim. Acta, Part A*. 188, 57-63 (2018). <https://doi.org/10.1016/j.saa.2017.06.041>
76. W. L. Zhang, Y. N. Zhao, Z. Z. Shi, D. Cong, Y. S. Bai, *J. Environ. Pathol. Toxicol. Oncol.* 37(4) (2018).
<http://doi.org/10.1615/JEnvironPatholToxicolOncol.2018027418>
77. V. Toragall, V. Baskaran, *Carbohydr. Polym.* 254, 117409 (2021).
<https://doi.org/10.1016/j.carbpol.2020.117409>

Figures

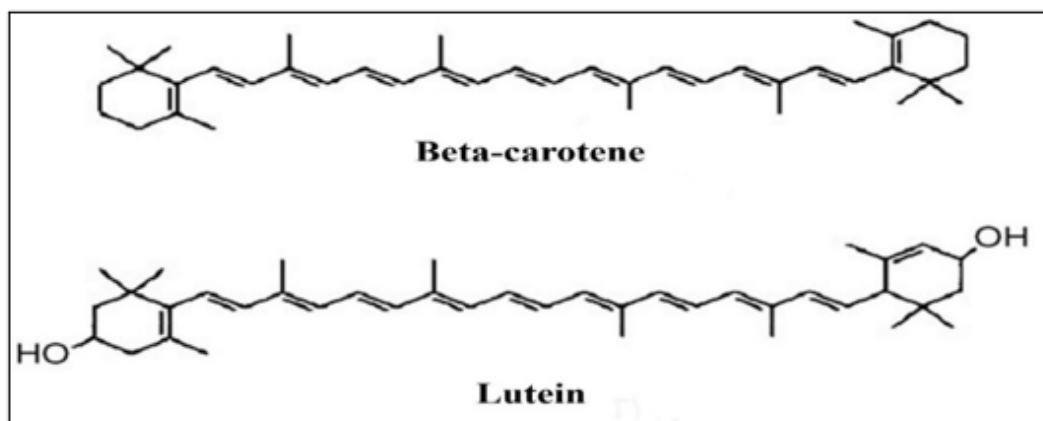


Figure 1

Beta carotene and Lutein chemical structure

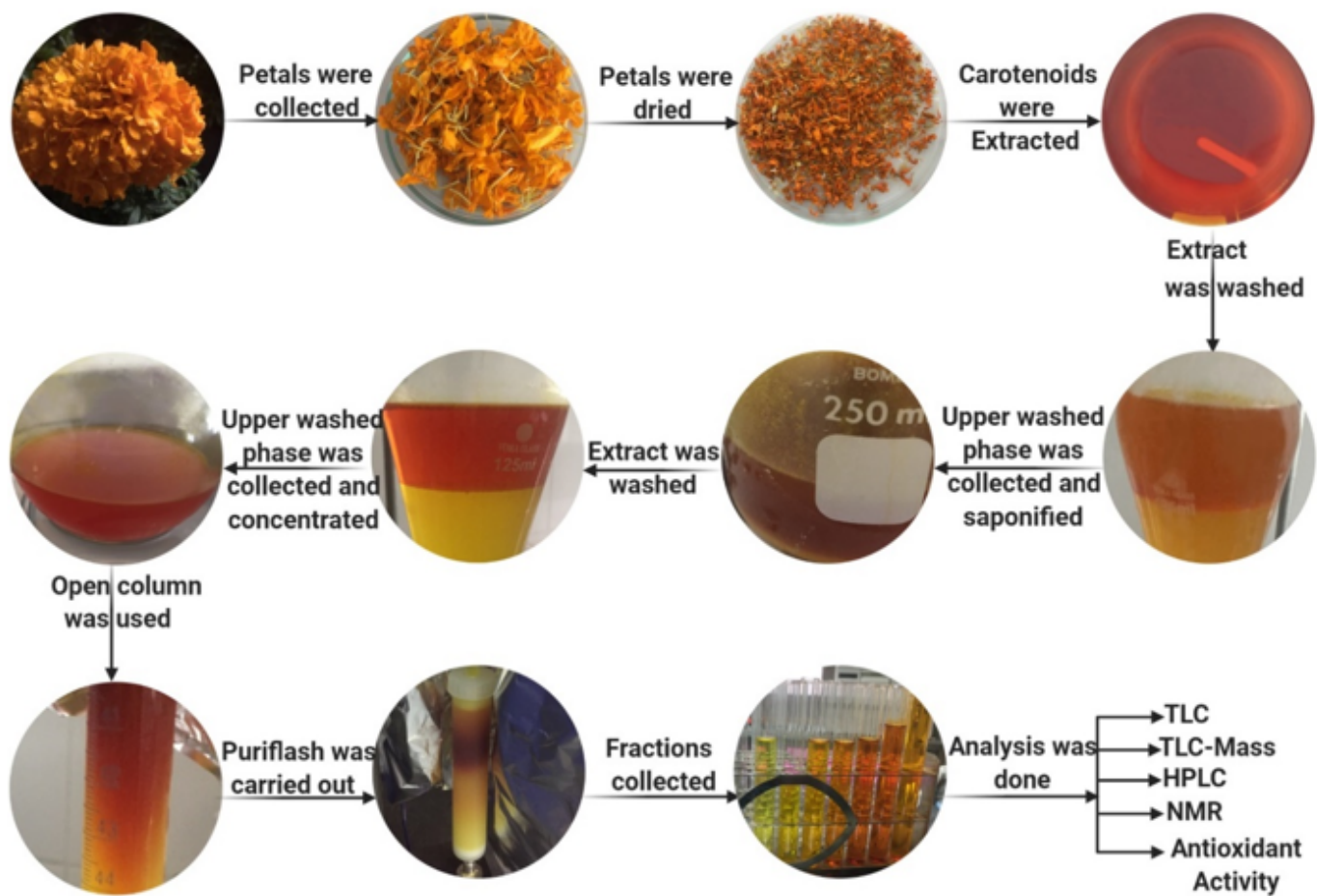


Figure 2

Procedures of extraction and purification of Lutein from Marigold flower

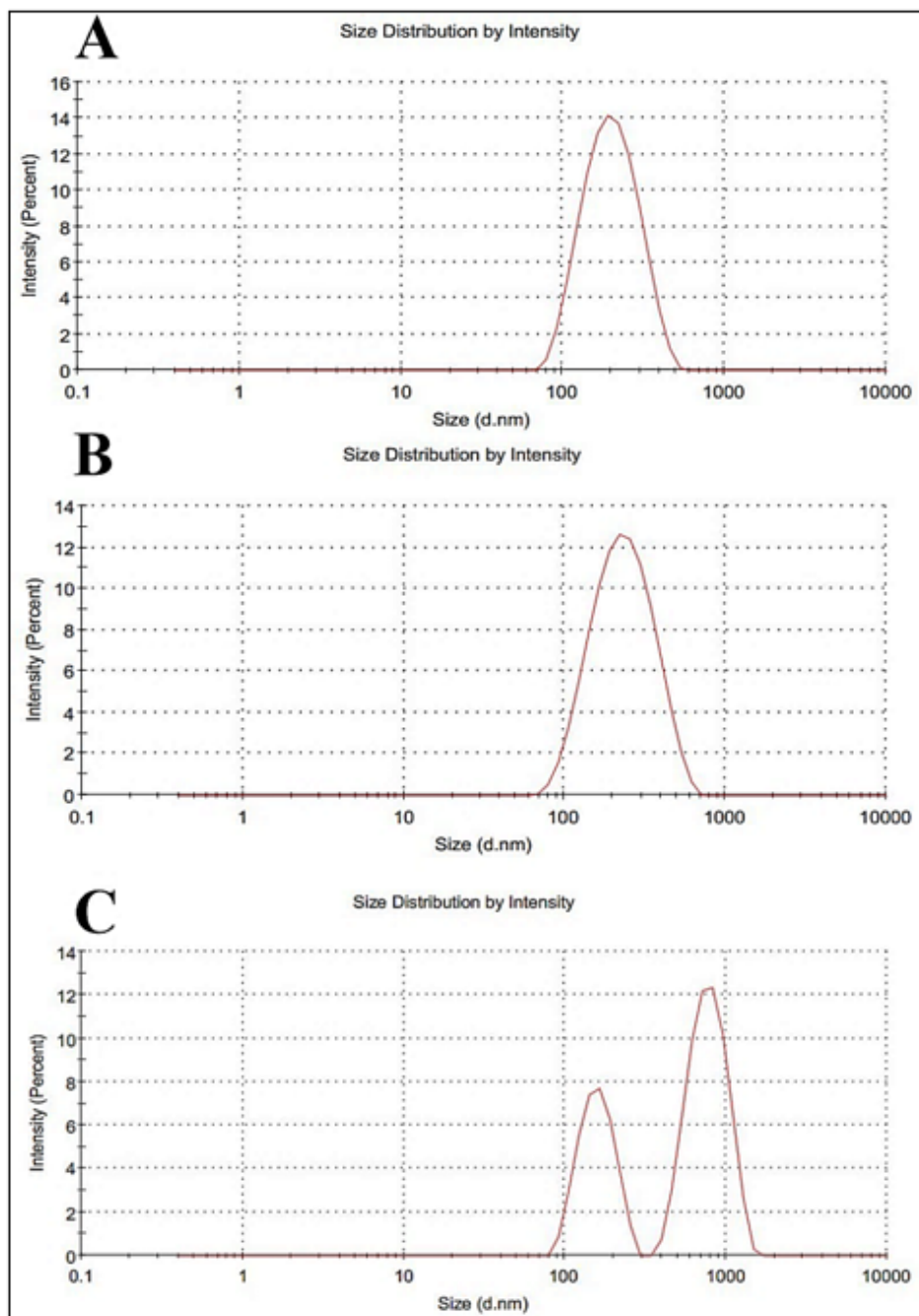


Figure 3

Size distribution of nanodispersions determined by dynamic light scattering (DLS) for Nano-Lut (A), Nano-SBc (B), and Nano-EBc (C).

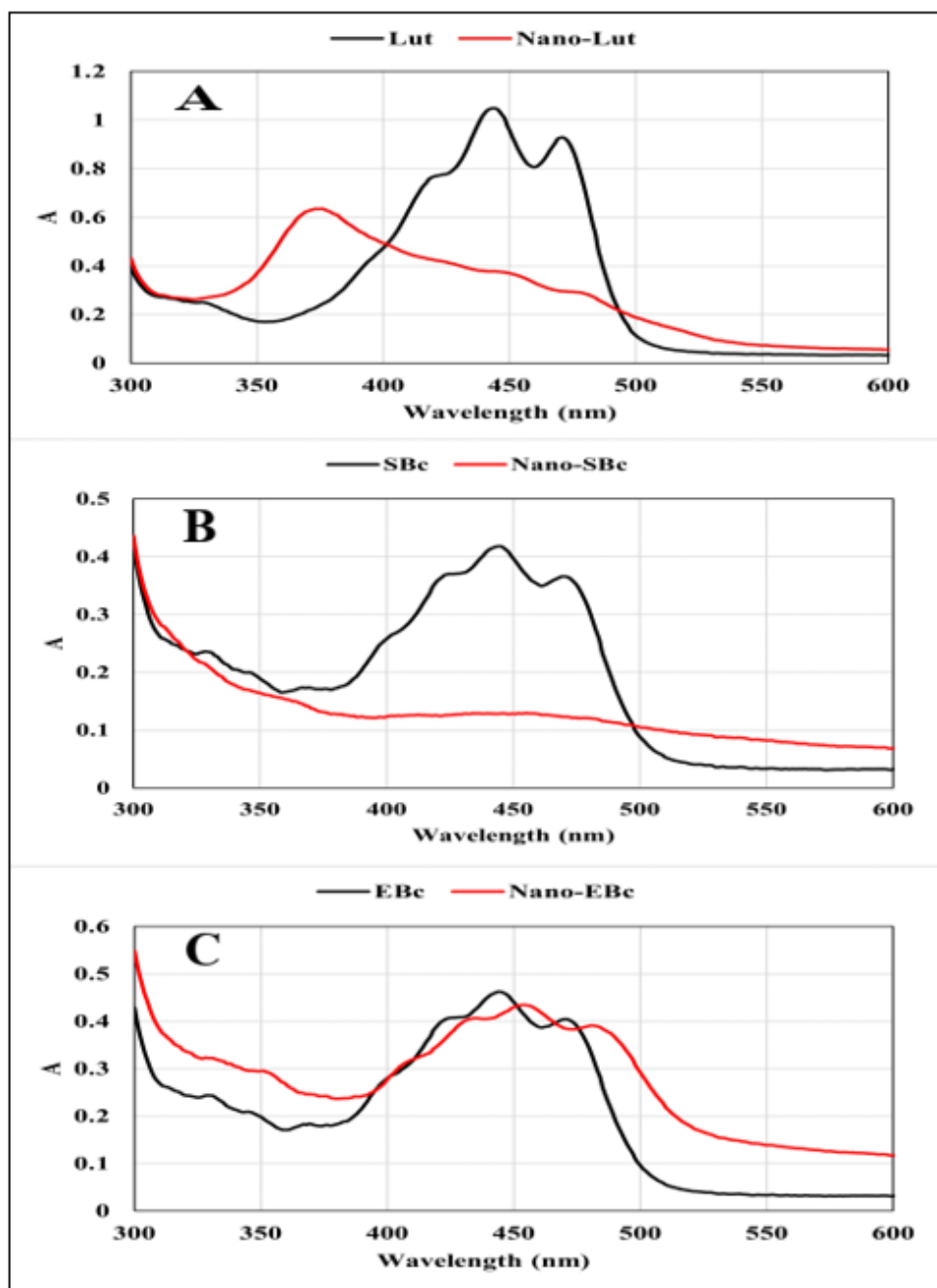


Figure 4

UV-Vis's spectra of Lut+Nano-Lut (A), SBc+Nano-SBc (B), and EBc+Nano-EBc (C).

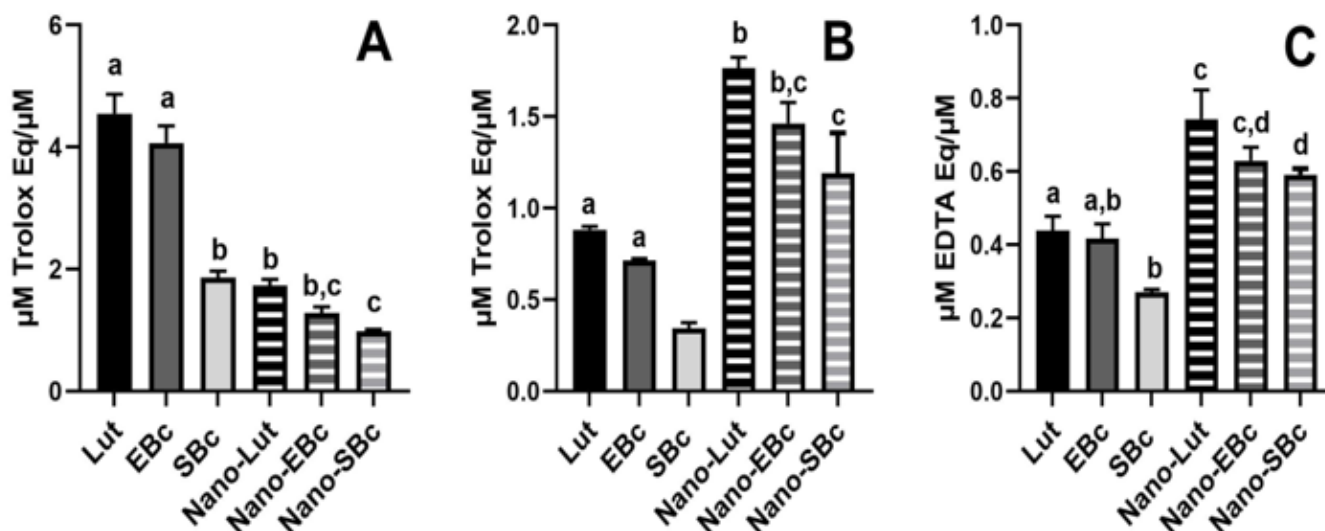


Figure 5

A: ABTS, B: FRAP, and C: Ferrozine activities of the different carotenoids and their nanodispersions forms as compared to standards in molar concentrations. Bars represent the average values with the standard deviations. Bars labeled with the same letter denote non-significant differences and those with different letters denote significant differences at $P < 0.05$.

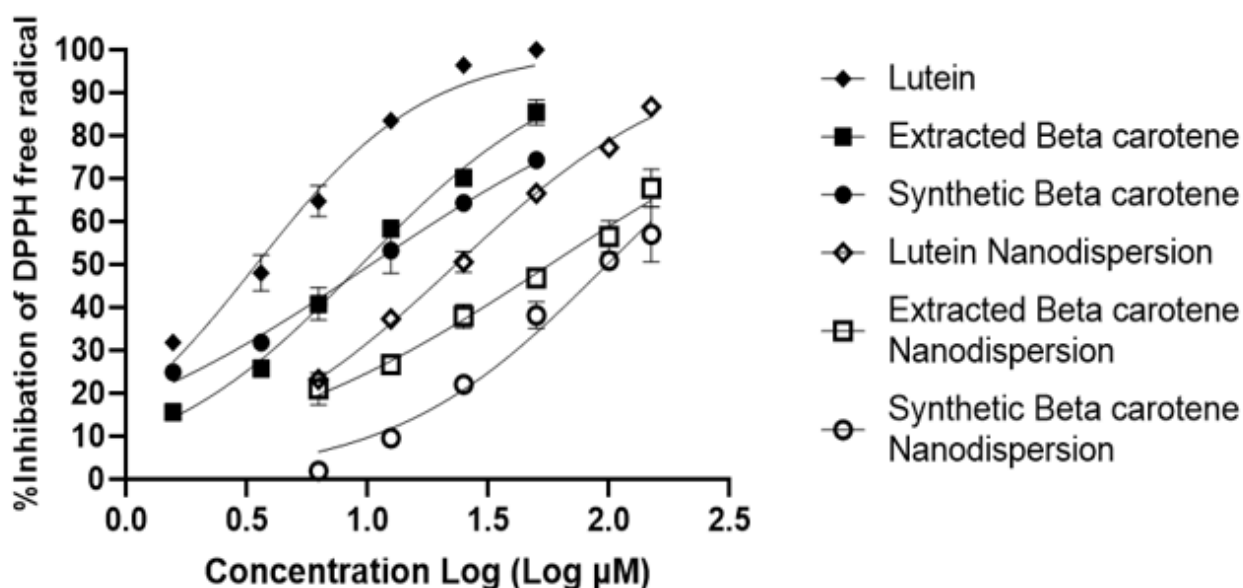


Figure 6

DPPH free radical inhibition curves achieved by different concentrations of the tested carotenoids and their nanodispersions. X-axes represent the logarithmic value of the effective concentration while the y-axis represents the average % of free radical inhibition \pm SD.

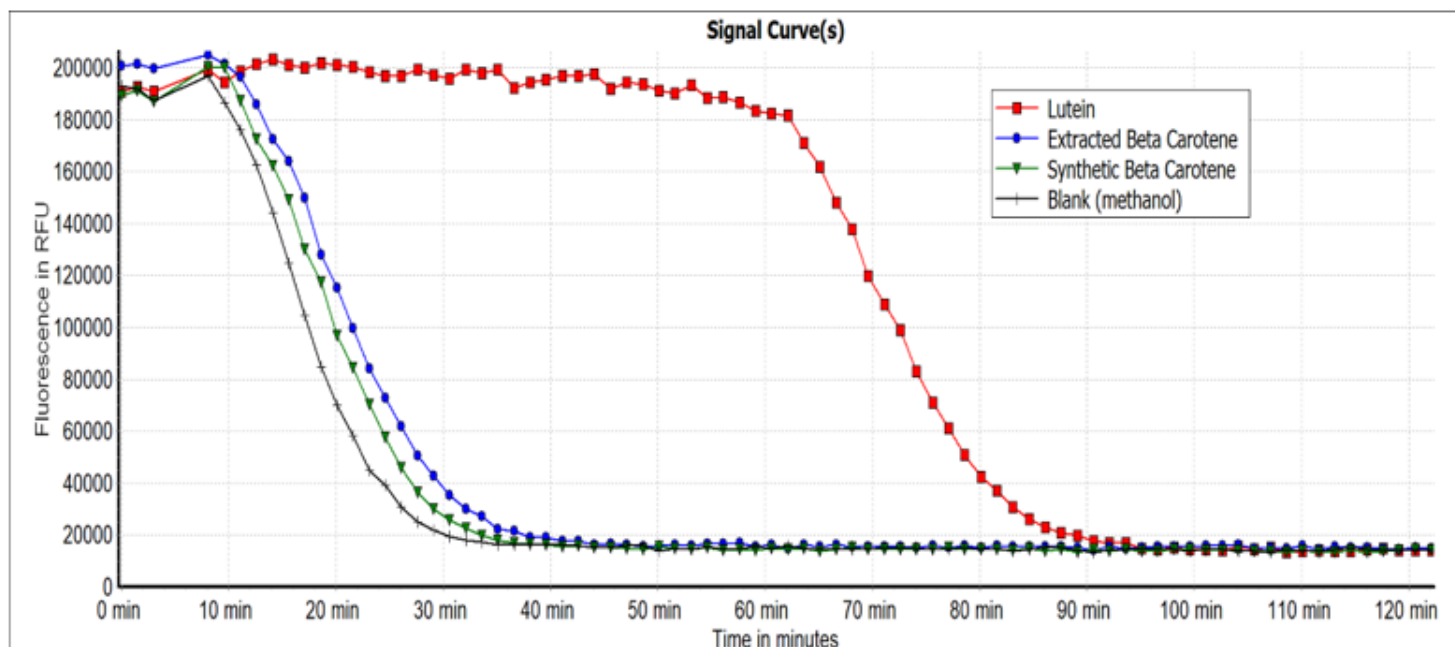


Figure 7

Fluorescein oxidative decay curves for 120 minutes achieved when applying 50 μ M effective concentration of the three carotenoids. The delayed decay increases the area under the curve, and this indicates better antioxidant capacity.

Supplementary Files

This is a list of supplementary files associated with this preprint. Click to download.

- [Supplementary.docx](#)